11th World Congress on Computational Mechanics (WCCM XI)
5th European Conference on Computational Mechanics (ECCM V)
6th European Conference on Computational Fluid Dynamics (ECFD VI)
E. Oñate, J. Oliver and A. Huerta (Eds)

SIMULATION OF SEMIDILUTE SUSPENSIONS BY DISSIPATIVE PARTICLE DYNAMICS

ABOUZAR MOSHFEGH†, AHMAD JABBARZADEH†,*

† School of Aerospace, Mechanical and Mechatronic Eng., The University of Sydney, NSW 2006, Australia. E-mail: ahmad.jabbarzadeh@sydney.edu.au.

Key Words: *DPD, Colloidal Suspension, Parameterisation, Semidilute Regime.*

Abstract. The stochastic Dissipative Particle Dynamics (DPD) method is calibrated to discover how relative viscosity of monodisperse colloidal suspension versus volume fraction behaves against different settings assumed for solid mesoparticles. This process together with monitoring the system statistical properties and temperature reveals routes towards capturing the experimental relative viscosity with reasonable computational cost and numerical complexity. Amongst many setting parameters, we only focus on alteration patterns in relative viscosity in semidilute regime obtained by changing solid DPD particles diameter, repulsion coefficient and dissipation rate. Repulsion parameter for solid species plays a major role in adjusting system homogeneity which is crucial to have a stable suspension by avoiding agglomeration. An interesting connection is made between the degree of suspension homogeneity, 3D occupancy patterns and maximum peak in radial distribution function (RDF). The isotropy in diffusion patterns and MSD linear graphs assist to obtain the optimum species size ratio leading to experimental relative viscosity.

1 INTRODUCTION

Suspensions contain dispersed particles within the range of 10 nm to 1 μm which reasonably fall in mesoscale range. Therefore, Dissipative Particle Dynamics (DPD) mesoscopic method[1,2] has been utilised widely to study colloidal suspensions. The off-lattice DPD method offers the coarse-graining ability that facilitates the multiscale simulation of suspensions where background solvent and suspending solutes differ in relaxation time and length scale. First attempts in suspension analysis were made by Koelman and Hoogerbrugge[3], and then suspensions including spheres, rods and disks were studied by Boek *et al.*[4] to explore the shape and size of suspending particles on rheology. They found DPD as a suitable alternative to continuum-based approaches like Brownian Dynamics or Stokesian Dynamics methods. Whittle and Dickinson[5] reported that bigger size of colloidal particles can enhance the hydrodynamic interaction in suspension. In 2006, Chen *et al.* emphasised on the importance of DPD dissipation rate on the drag force and torque calculated for an immobilised DPD particle[6]. Martys[7] captured the experimental relative viscosity in very dilute and semidilute regimes in a big simulation box of volume of 45^3 (DPD units) and particle-to-solvent size ratio of 11.022. Then he included the lubrication force to avoid particles overlap in dense suspensions. Pan *et al.*[8] proposed a hybrid conservative force to perfectly represent a colloidal particle by a single DPD particle where colloid rotational

degree of freedom was taken into account. Colloids size was taken 5.511 times bigger than solvent particles. They introduced the exponential pairwise conservative potentials as the key factor to prevent probable aggregation of colloidal particles. It will be shown later that repulsion coefficient between colloidal particles plays the same preventive role by tuning the intensity of agglomeration.

In this study, contrary to prevalent approach in DPD simulations, we are interested to perform sensitivity analyses to find the hidden and non-monotonic correlations between DPD input parameters and simulation results. The study focuses on the solid mesoparticles setting parameters including the inter-repulsion coefficient, species size ratio and dissipation rate. System statistics, temperature and relative viscosity are monitored rigorously to guarantee that experiment has been captured correctly. 3D system snapshots, colloids occupancy pattern, radial distribution function, and isotropy of diffusion coefficients are all scrutinised to achieve a set of optimum setting parameters.

2 PHYSICS AND FORMALISM

2.1 DPD governing equations

The spatiotemporal evolution of each DPD particle is integrated by Newton's second law of motion in a Lagrangian particle tracking approach via:

$$d\boldsymbol{r}_i = \boldsymbol{v}_i\,\Delta t\,, \qquad d\boldsymbol{v}_i = \frac{\boldsymbol{F}_i}{m_i} = \frac{1}{m_i}\sum_{j\neq i}\boldsymbol{F}_{ij}\,\Delta t\,, \qquad \boldsymbol{F}_{ij} = \boldsymbol{F}_{ij}^{C} + \boldsymbol{F}_{ij}^{D} + \boldsymbol{F}_{ij}^{R} \tag{1}$$

where $(\boldsymbol{r}_i,\boldsymbol{v}_i)$ are respectively the position and velocity vectors of indexed i^{th} particle in Cartesian coordinate, Δt is the simulation time step, m_i is the particle mass and the vector $\boldsymbol{F}_{ij}$ stands for all kinds of pairwise interparticle forces applied from j^{th} particle, and $\boldsymbol{F}_i$ is the vector sum of all forces applied on i^{th} particle. This encompasses three pairwise-additive major DPD forces known as conservative ($\boldsymbol{F}_{ij}^{C}$), dissipative ($\boldsymbol{F}_{ij}^{D}$) and random ($\boldsymbol{F}_{ij}^{R}$) forces. Common form of deterministic conservative force is given by:

$$\boldsymbol{F}_{ij}^{C} = A_{ij}\omega^{C}(r_{ij})\,\frac{\boldsymbol{r}_{ij}}{r_{ij}} = A_{ij}\left(1-\frac{r_{ij}}{R_c}\right)\frac{\boldsymbol{r}_{ij}}{r_{ij}}. \tag{2}$$

where $\boldsymbol{r}_{ij}$ is interparticle distance vector, A_{ij} is the repulsion parameter adjusting the repulsive strength and can be set differently for each species, R_c is the cutoff radius (or particle effective diameter) and DPD length scale beyond which the interparticle repulsive interactions are turned off, and $\omega^{C}(r_{ij})$ is the weight function for this force. The pairwise random force stochastically compensate the lost degrees of freedom due to coarse-graining.

$$\boldsymbol{F}_{ij}^{R} = \sigma_{ij}\,\omega^{R}(r_{ij})\,\frac{\xi_{ij}}{\sqrt{dt}}\,\frac{\boldsymbol{r}_{ij}}{r_{ij}}, \tag{3}$$
$$\langle\xi_{ij}(t)\rangle = 0 \quad and \quad \langle\xi_{ij}(t)\,\xi_{kl}(t')\rangle = (\delta_{ik}\delta_{jl}+\delta_{il}\delta_{jk})\,\delta(t-t'),$$

Here, $\omega^{R}(r_{ij})$ is the weight function, σ_{ij} is the noise amplitude for randomly generated numbers (ξ_{ij}) with Gaussian white-noise statistics, zero mean and unit variance. They are uncorrelated for different pairs of particles while holding in the relation ($\xi_{ij}=\xi_{ji}$) to maintain centrality of pairwise force. In this paper we adopt an alternative and use the *Mersenne*

Twister pseudorandom numbers generator[9] to yield double precision equidistributed uniform numbers (θ_{ij}) between 0 and 1:

$$\xi_{ij} \approx \sqrt{12}\,(\theta_{ij} - 0.5). \tag{4}$$

This distribution not only resembles Gaussian distribution but also excels in computational efficiency. The viscous resistance is modelled by dissipative force varying as a function of inter-particle relative velocity, it reads:

$$\boldsymbol{F}_{ij}^{D} = -\gamma_{ij}\,\omega^{D}(r_{ij})\,(\boldsymbol{r}_{ij}\cdot\boldsymbol{v}_{ij})\,\frac{\boldsymbol{r}_{ij}}{{r_{ij}}^{2}}. \tag{5}$$

where $\omega^{D}(r_{ij})$ is the weight function, γ_{ij} is the damping factor or drag coefficient between particles species i and j, and $\boldsymbol{v}_{ij}$ is the relative velocity between two indexed particles. The negative sign indicates that this force is the only force which decelerates particles motion. The combination of dissipative and random forces creates a DPD thermostat enabling the system to reach a guaranteed equilibrium[2]. Stationary solution to the Fokker-Planck equation in form of Gibbs function is achieved only when dissipation-fluctuation theorem is satisfied in equilibrium temperature T via the following relation[1]:

$$\omega^{R}(r_{ij}) = \left[\omega^{D}(r_{ij})\right]^{1/2}, \quad \sigma = (2\,k_B T\,\gamma\,)^{1/2}. \tag{6}$$

where k_B is the Boltzmann constant. This suggests that one of the weight functions in dissipative or random force can be opted arbitrarily.

$$\omega^{D}(r_{ij}) = \left[\omega^{R}(r_{ij})\right]^{2} = \begin{cases} \left(1 - \dfrac{r_{ij}}{r_c}\right)^{2}, & r_{ij} < r_c \\ 0, & r_{ij} \geq r_c \end{cases} \tag{7}$$

The $(\boldsymbol{F}_{ij}^{D}, \boldsymbol{F}_{ij}^{R})$ forces act along the line of centres and conserves both linear and angular momenta[10].

2.2 Auxiliary formulations

The emphasis is on the linear Couette flow as a successful numerical viscometer via Lees-Edwards boundary condition[11]. The DL-Meso adopts the modified Lees-Edwards shearing method as articulated by Chatterjee[12] which minimises the numerical artefacts in form of abrupt jumps in velocity profiles near shear boundaries. The modified version attempts to avoid thermalising the particles crossing the shear boundaries via DPD thermostat. Relative viscosity is then obtained by dividing the viscosities calculated for suspension and solvent individually via $\eta = -S_{xy}/\dot{\gamma}$ where numerator is the shear stress and denominator stands for shear rate[1]. There have been several methods to calculate the volume fraction of solid particulates in suspension in which the radius assigned to colloidal particles differs. Among using the hydrodynamic radius out of Stokes-Einstein relation of diffusion, effective diameter based on peak in RDF graph, and cutoff radius set for solid particles we pick up the last method as used in Martys' work[7]. It reads:

$$\phi = \frac{N_p V_p}{V_{box}} \quad where \quad V_p = \frac{4}{3}\pi R_c^3 \tag{8}$$

where V_{box} is the volume of cubic simulation box. In this study we decided to match the density ratio between solvent and solid mesoparticles to de Kruif *et al.* experiment[13], therefore the below formula is used to find the solid particle mass (M_p):

$$M_p = M_s * \frac{\rho_p}{\rho_s} * \left(\frac{R_p}{R_s}\right)^3 \tag{9}$$

Here, subscripts p and s refer to particles and solvent respectively, M is the mass, ρ stands as the species density in nature and R represents the radius of DPD particle.

3 RESULTS AND DISCUSSION

We believe that in order to capture experiment by the stochastic DPD method, one should not expect predictable monotonic correlation between setting parameters and simulation outputs. Nevertheless, this does not mean that exploring a clear and smooth correlation is beyond possibility. Hence, the need for numerical calibration as defined further becomes even more prominent. The calibration scenario begins by a set of setting parameters as a computationally inexpensive case and then altering parameters individually to see how crucial outputs respond. Convergence of system total energy as equilibrium criterion, temperature as a testament for acceptable thermostating, and relative viscosity of suspension compared with experiment are valuable outputs to guarantee the calibration.

To examine present calibration method on a firm rheological basis, we focus this study on semidilute colloidal suspensions ($\phi \leq 0.2$) consisting of two species: the solvent particles and solid mesoparticles. As a result of an unsystematic calibration to get experimental behaviour with reasonable computational cost at ϕ = 0.193, the following optimum case was obtained which counts as foundation for an organised calibration in this work: V_{box} = 10^3, Δt= 0.01, total time steps N_t= 50,000, solvent-solvent repulsion coefficient A_s=18.75, γ_s= 50, ρ_s= 4, number of solvent particles N_s= 4000, d_s= 1, M_s= 1, V_s= 1, M_p=9.33, d_p=1.75, A_p=3500 and γ_p= 4.5. We aim to match our rheological results to experiment on the basis of relative viscosity reported in de Kruif *et al.*[3] where silica particles with density of 1.74 kg/m^3 suspend in an oily solution of cyclohexane without active electrostatic interactions. Data production starts after 40,000 time steps and lasts for the remnant 10,000 time steps. System statistics, temperature and relative viscosity are investigated in a range of varying repulsion coefficient (A_p) of solid particles, mesoparticles diameter (d_p) and dissipation rate between solid particles (γ_p). Morphological diversity in mesoparticles occupancy patterns plays the key role to classify degrees of homogeneity as major criterion to have a stable suspension.

3.1 Repulsion coefficient (A_p)

Among the relevant DPD setting parameters, we found repulsion coefficient of solid mesoparticles (A_p) very effective to adjust their spatial spacing in an equilibrated simulation. As backed by Flory-Huggins theory[10], repulsion coefficient of suspending species is closely related to its solubility which characterises the intensity that mesoparticles tend to scatter thorough the solvent.

Snapshots of solid mesoparticles in the last time step are depicted in Fig. 1 for A_p values changing from 18.75 (same as solvent) to 3500. The particles travel in the form of aggregates so that their relative positions remain relatively constant. Qualitatively speaking, for A_p <75 a fairly dispersed solid phase is observed, while for 75≤ A_p <2000 homogeneity deteriorates and particles form discernible aggregates. This trend is conversed for 2000≤ A_p ≤3500 where interparticle repulsion is strong enough to avoid agglomeration and approach the system to experimental behaviour at the same time.

We need more quantitative tools such as RDF graphs and system relative viscosity (η_r) to come up with an optimum A_p value. Fig. 2 renders radial distribution function plotted for solvent particles in which no fundamental difference is apparent when A_p alters. RDF graphs are then plotted for solid mesoparticles without inclusion of solvent particles in Fig. 3 to connect them with observed bimodal behaviour between A_p and agglomeration. The major discrepancy between RDF graphs is the magnitude of abrupt peak in population density which is intensified as A_p increases from 18.75 to 500 as shown in Fig. 3 (a). This correlation is reversed when A_p exceeds 500 so that increasing A_p reduces the maximum concentration occurred in RDF (see Fig. 3 (b)). It is simply inferred that A_p= 500 is the turning point in this bimodal behaviour, a fact not recognisable from snapshots (Fig. 1). Another noticeable point is the obvious reduction in DPD particles softness up to r/r_c = 1 (as opposed to solvent RDF shown in Fig. 2) which reflects the transition from soft DPD beads to relatively hard spheres for solid mesoparticles.

Maximum RDF versus repulsion coefficient is diagrammed in Fig. 4 to support this bell-shaped trend with turning point at A_p=500. Solid particles behave rather similar to solvent at small values of A_p due to equal repulsion. Higher RDF values denote greater spatial concentration of mesoparticles and therefore less homogeneity across the system. This leads to an unstable suspension which we intend to avoid from in the present study. We concluded that to avoid prominent heterogeneity or agglomeration, two conditions must be met. First, RDF for solid particles should vary in the same scale as solvent. Secondly, the density distribution for solid particles across the sheared domain should be as uniform as possible.

The suspension relative viscosity and its deviation percentage from experiment (1.76≤ η_r ≤2 at ϕ=0.191)[13] are plotted versus A_p in Fig. 5 based on η_{exp}=1.8. System static temperature is also histogrammed over the ranges of A_p studied. At small repulsion coefficients, the solid mesoparticles hydrodynamics resembles the solvent and therefore they both manifest similar viscosities ($\eta_r \approx 1$). Increment of interparticle repulsive force not only cools down the suspension temperature but also approaches the relative viscosity to experiment. In conclusion, it was realised that repulsion intensity affects the suspension hydrodynamics and at some stages can cause significant agglomeration. It is crucial to find an optimum value such as A_p=3500 by maintaining the RDF peaks at reasonable scales to avoid aggregate formation, and monitoring the suspension snapshots, system relative viscosity and temperature.

3.2 Species size ratio (d_p/d_s)

Due to incredibly higher population of solvent particles, they are coarse-grained while the solid particles are meant to represent actual mesoparticles. Therefore, coarse-graining prevents us to have a clear size ratio between two species since it is not adaptable to size ratios observed in reality. Even though a variety of size ratios are utilised in literature such as d_p/d_s=5.5 [7], d_p/d_s= 5 [14] and d_p/d_s= 3.6 [8], we believe there is no definite choice. Instead, suspension microstructure and the type of intended rheology and relative viscosity dictate the appropriate size ratio at which correct simulation statistics are obtained. Regarding the solvent particles diameter set to unity in setting parameters of optimum case as introduced, the size ratio (d_p/d_s) or solid particles size (d_p) varies from 1 to 5 in this study.

3.2.1 Diffusion patterns

The radial distribution function peaks roughly at unique radius ranges of $r/\mathrm{r}_c \sim$ 0.82-0.89 and $r/\mathrm{r}_c \sim$ 1.005-1.09 respectively for solvent and solid particles regardless of d_p value chosen.This conveys the fact that RDF is mostly affected by repulsion coefficient not the species size ratio. Therefore, the calibration process in this section relies on diffusion of solid mesoparticles rather than the RDF. Complicated measures must be taken to calculate the diffusion coefficient in the direction where streaming velocity dominates the particles transport. Hence, the diffusion coefficient is calculated for both species in y and z directions perpendicular to linear streaming velocity. Fig. 6 contains D_z and D_y diffusion coefficients plotted over the size ratio range $1 \leq d_p/d_s \leq 5$ for solvent and solid species. In Fig. 6 (a), solvent particles almost adhere to a unique diffusion pattern along both studied directions except at d_p/d_s= 1. In Fig. 6 (b), the solid mesoparticles show relatively constant and equal D_z and D_y diffusion coefficients (~0.2) for $1.4 \leq d_p/d_s \leq 3.5$ while sort of asymmetric diffusion is apparent out of this range. It shows that colloidal particles diffuse almost similarly and uniformly in y and z directions which proves that suspension homogeneity stays isotropic for these size ratios. Other prominent feature is convergence of solvent diffusion components to unity which shows that solvent diffusive behaviour is left rather intact for $4 \leq \mathrm{d_p}/\mathrm{d_s} \leq 5$. This is because of reduced number of solid particles influencing the solvent as species size ratio rises. It was decided not to bring the Mean Square Displacement (MSD) for simplicity since diffusion graphs express the same message. The best correspondence between y and z diffusion and also MSD linear graphs takes place at d_p=1.75 as shown by a circle as the optimum size ratio to yield isotropic diffusion and homogeneity. For $1.0 \leq d_p/d_s \leq 1.75$, plotted density profiles for both solid and liquid phases shows uneven concave and convex extremisms as a result of mesoparticles agglomeration. This phenomenon influences the velocity profile accordingly and deforms its linearity to curvature. In general, as d_p increases from 1 to 1.75 these anomalous behaviours are all rectified and density profiles become horizontal and linear velocity profiles are achieved. Further increase in d_p value accompanies by increasing erratic fluctuations in density profile for solid particles only, while the liquid density profile and velocity profile behave still naturally.

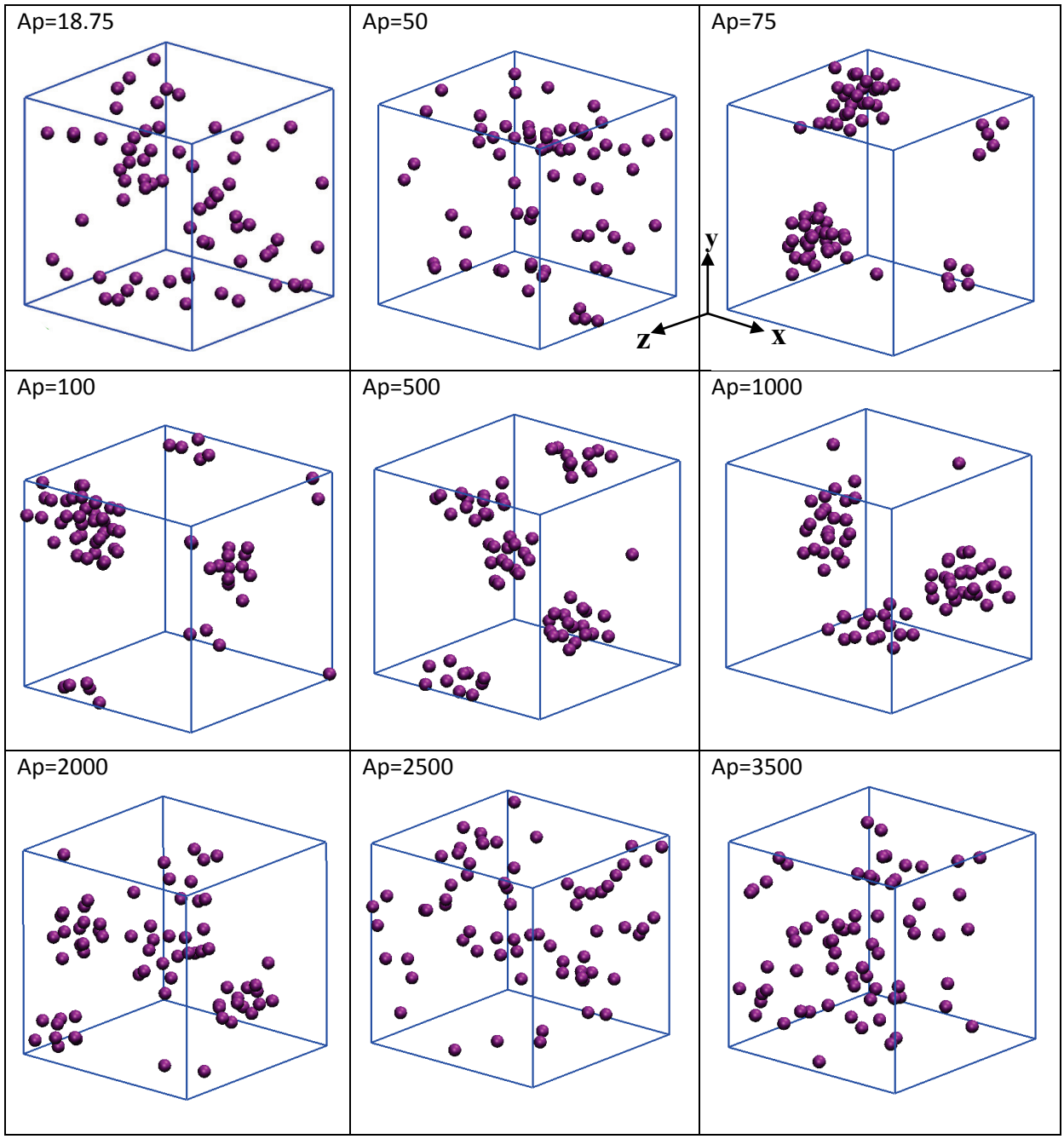

Figure 1: Snapshots of equilibrated solid mesoparticles at last time step versus different repulsion coefficients, $18.75 \leq A_p \leq 3500$.

3.2.2 Temperature and rheological aspect

Deviation percentage of calculated relative viscosity (η_r) from experimental values in the range of studied mesoparticles sizes are shown in Fig. 7. The absolute relative viscosity and system static temperature are also appended for clarity. Gradual decrement in suspension relative viscosity is the dominant trend as solid particles get bigger. For $3.5 \leq d_p/d_s \leq 5$,

relative viscosity becomes independent of species size ratio. This means that the simulated system behaves differently from the actual suspension in which η_r is very sensitive to solid particles size. Temperature assists greatly to spot the optimum species size ratio so that

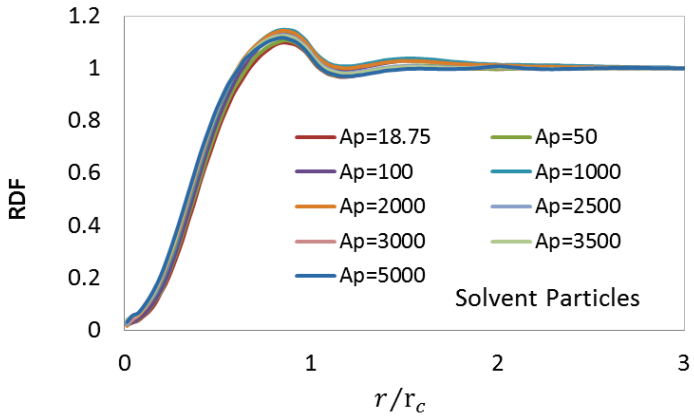

Figure 2: Radial distribution function dedicated to solvent particles plotted across studied repulsion coefficients.

minimum system temperature occurs exactly at the point where least deviation of η_r from experiment takes place, say d_p/d_s=1.75. An abrupt jump in both relative viscosity and temperature is observed for $1.1 \leq d_p/d_s \leq 1.2$ where RDF of solid mesoparticles shows maximum concentration, i.e. agglomeration. Therefore, size ratio as well as the repulsion coefficient plays a key role to cause or prevent aggregates formation. The optimum size ratio, d_p/d_s=1.75, accompanies with lowest standard deviation or fluctuation in density profile of solid particles across the Couette flow.

A range of dissipation rates between solid particles, $4.5 \leq \gamma_p \leq 500$, was also taken under examination, but no meaningful and monotonic correlation between γ_p, relative viscosity and temperature was tracked. In fact, all the studied data points had less than 2% deviation from experimental values. The value of γ_p=4.5 was found as the best dissipation rate with relative viscosity of 1.818.

4 CONCLUSIONS

Dissipative particle dynamics method was calibrated against important DPD parameters for solid particles in order to capture the experimental behaviour in suspensions with least complexity and computational cost. Particle-Particle repulsion coefficient (A_p), species size ratio (d_p/d_s) and dissipation rate (γ_p) were taken under examination to clarify missing links between DPD setting parameters and aggregate formation, diffusion patterns, RDF, relative viscosity and temperature. The following conclusions were found noticeable as drawn:

- A bell-shaped behaviour was observed between repulsion coefficient (A_p) and peak magnitude in RDF graphs as a sign of agglomeration intensity of solid mesoparticles. For $18.75 \leq A_p \leq 500$, there exists direct relationship between A_p and agglomeration

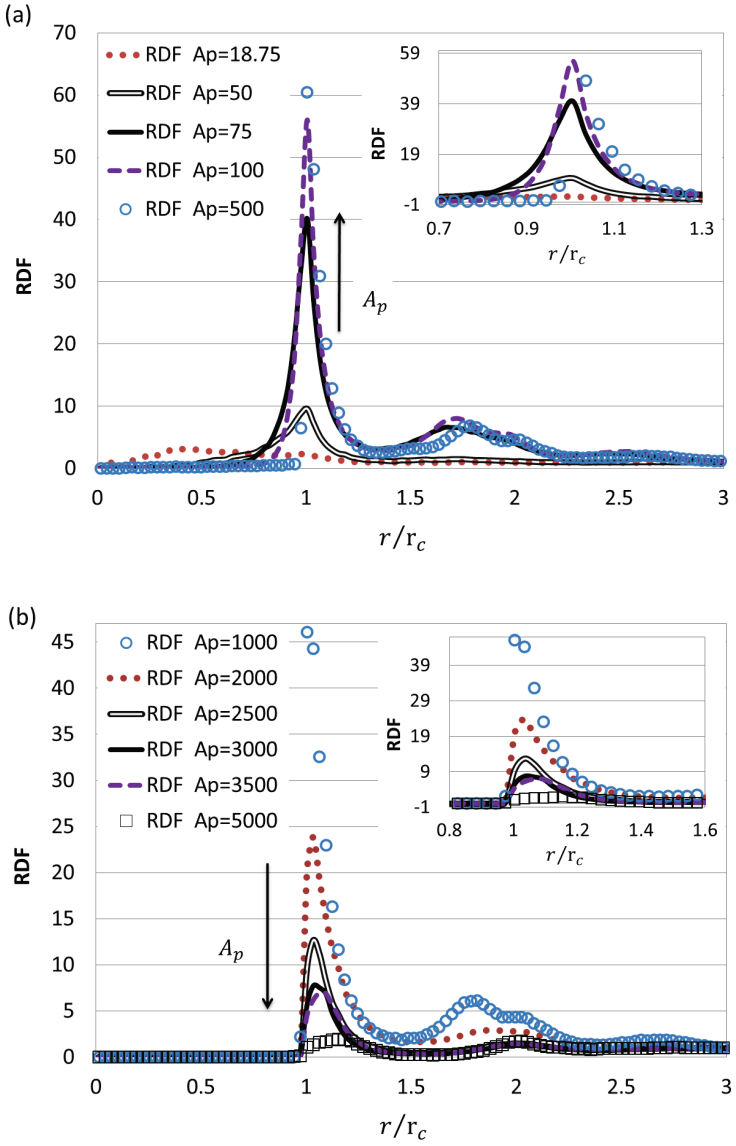

Figure 3: Radial distribution function dedicated to solid mesoparticles plotted across studied repulsion coefficients: part (a) 18.75 ≤ A_p ≤ 500; part (b) 1000 ≤ A_p ≤ 5000. The insets show the close-up view.

intensity while for 500≤ A_p ≤3500 it turns into indirect correlation. More specifically, for A_p <75 solid particles are fairly dispersed whereas for 75≤ A_p <2000 symptoms of heterogeneity arises, and afterwards intense agglomeration is restored to a homogeneous suspension where experiment is achievable.

- In the range of 18.75≤ A_p ≤5000, suspension relative viscosity increases from unity up to experimental value (η_{exp}=1.8) at optimum repulsion coefficient, A_p=3500. Temperature is also cooled down as A_p increment approaches the system viscosity to experiment.
- Spatial correlation of solid particles expressed by RDF is mostly affected by interparticle

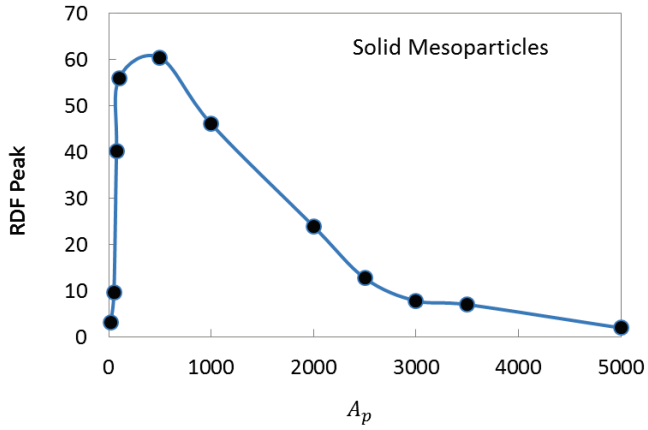

Figure 4: Maximum spatial concentration (RDF) of mesoparticles plotted against repulsion coefficient, 18.75 $\leq A_p \leq$ 5000.

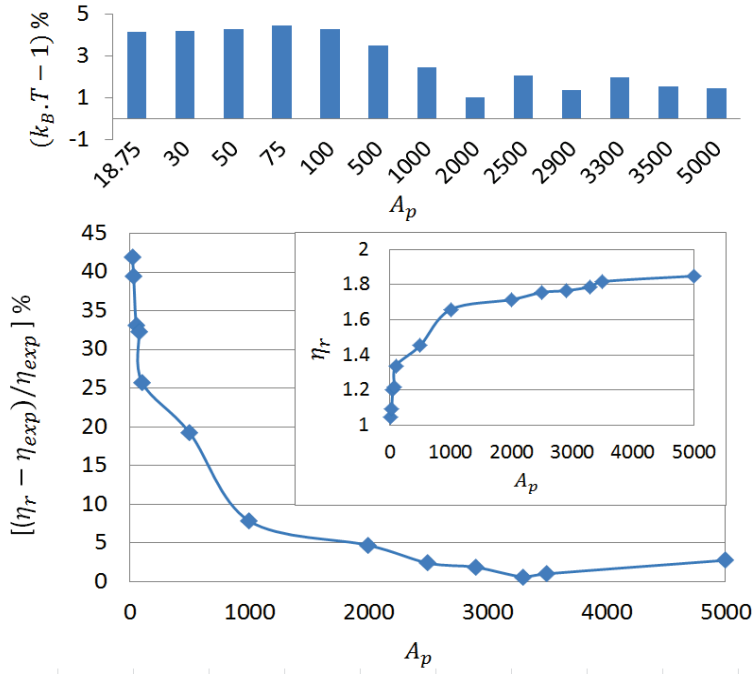

Figure 5: Deviation of system relative viscosity from experiment (η_{exp}=1.8) versus 18.75 $\leq A_p \leq$ 5000 together with system relative viscosity given as inset and histograms of temperature deviation from equilibrium.

repulsion rather than species size ratio. Diffusion coefficients, D_y and D_z, remain equally constant (~0.2) within 1.4$\leq d_p/d_s \leq$3.5 that proves the existence of an isotropic homogeneous suspension. The best correspondence between y and z diffusion and also MSD linear graphs takes place at optimum size ratio of d_p/d_s=1.75.

- A monotonically declining correlation between η_r and species size ratio was tracked in which independence of relative viscosity from mesoparticle size happens in3.5 $\leq d_p/d_s \leq$5. System temperature minimises at d_p/d_s=1.75 where experimental

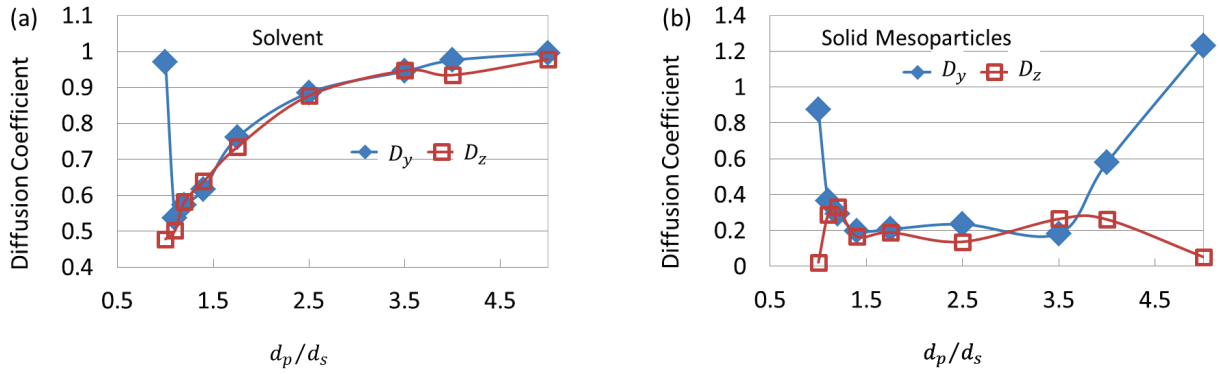

Figure 6: Variation of diffusion coefficient along y and z directions over the range $1 \leq d_p/d_s \leq 5$: Part (a) solvent; Part (b) solid mesoparticles.

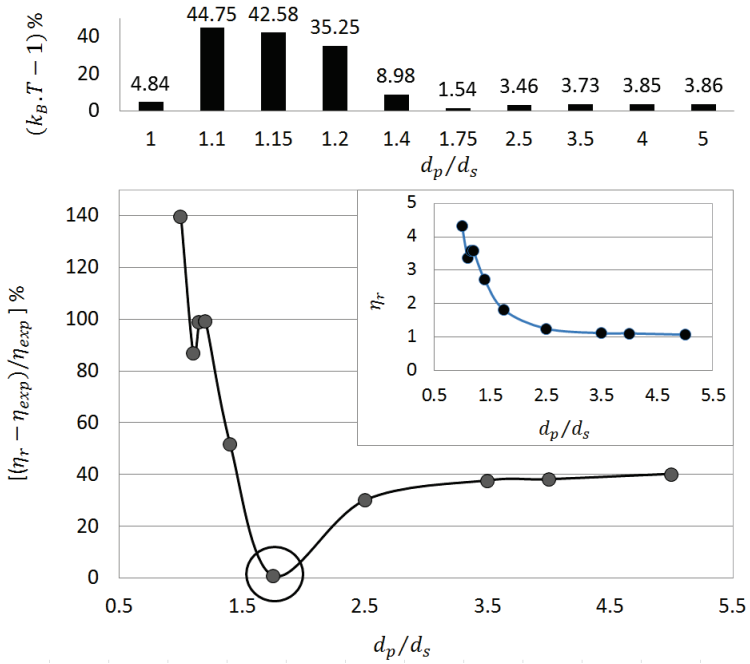

Figure 7: Deviation of system relative viscosity from experiment (η_{exp}=1.8) versus $1 \leq d_p/d_s \leq 5$ together with system relative viscosity given as inset and histograms of temperature deviation from equilibrium.

viscosity value is reached at the same time.

5 ACKNOWLEDGEMENTS

The present numerical simulation was accomplished by DL_Meso_DPD open source package[13] DL_MESO is a mesoscale simulation package written by R. Qin, W. Smith and M. A. Seaton and has been obtained from STFC's Daresbury Laboratory via the website http://www.ccp5.ac.uk/DL_MESO. The package was developed to add new post-processing tools to calculate radial distribution function and diffusion coefficient for each species. We also acknowledge the support of an *ARC Discovery* grant (for the second author), and *USydIS* scholarship (for first author). Computational times granted by Intersect Australia Ltd and also

Australian National Computational Infrastructure Facility for parts of calculations are thankfully acknowledged.

REFERENCES

[1] Español, P., & Warren, P. Statistical Mechanics of Dissipative Particle Dynamics. *EPL (Europhysics Letters),* (1995) **30:** 191-196.

[2] Hoogerbrugge, P. J., & Koelman, J. M. V. A. Simulating Microscopic Hydrodynamic Phenomena with Dissipative Particle Dynamics. *EPL (Europhysics Letters)* (1992) **19**: 155-160.

[3] Koelman, J., & Hoogerbrugge, P. Dynamic simulations of hard-sphere suspensions under steady shear. *EPL (Europhysics Letters)* (1993) **21:** p363.

[4] Boek, E., Coveney, P., Lekkerkerker, H., & van der Schoot, P. Simulating the rheology of dense colloidal suspensions using dissipative particle dynamics. *Physical Review E* (1997) **55:** 3124-3133.

[5] Whittle, M., & Dickinson, E. On simulating colloids by dissipative particle dynamics: Issues and complications. *Journal of Colloid and Interface Science* (2001) **242**: 106-109.

[6] Chen, S., Phan-Thien, N., Khoo, B. C., & Fan, X. J. Flow around spheres by dissipative particle dynamics. *Physics of Fluids (1994-present)* (2006) **18:** 103605-103619.

[7] Martys, N. S. Study of a dissipative particle dynamics based approach for modeling suspensions. *Journal of Rheology (1978-present)* (2005) **49**: 401-424.

[8] Pan, W., Caswell, B., & Karniadakis, G. E.. Rheology, Microstructure and Migration in Brownian Colloidal Suspensions. *Langmuir* (2009) **26:** 133-142.

[9] Matsumoto, M., & Nishimura, T. Mersenne twister: a 623-dimensionally equidistributed uniform pseudo-random number generator. *ACM Transactions on Modeling and Computer Simulation (TOMACS)* (1998) **8:** 3-30.

[10] Groot, R. D., & Warren, P. B. Dissipative particle dynamics: Bridging the gap between atomistic and mesoscopic simulation. *The Journal of Chemical Physics* (1997) **107:** 4423-4435.

[11] Lees, A., & Edwards, S. The computer study of transport processes under extreme conditions. *Journal of Physics C: Solid State Physics* (1972) **5**: 1921-1929.

[12] Chatterjee, A. Modification to Lees–Edwards periodic boundary condition for dissipative particle dynamics simulation with high dissipation rates. *Molecular Simulation* (2007) **33:** 1233-1236.

[13] de Kruif, C. d., Van Iersel, E., Vrij, A., & Russel, W. Hard sphere colloidal dispersions: Viscosity as a function of shear rate and volume fraction. *The Journal of Chemical Physics* (1985) **83:** 4717-4725.

[14] Schunk, P. R., Pierce, F., Lechman, J. B., Grillet, A. M., Veld, P. J. i. t., Weiss, H., Stoltz, C., Heine, D. R. Performance of mesoscale modeling methods for predicting rheological properties of charged polystyrene/water suspensions. *Journal of Rheology* (2012) **56:** 353-384.

[15] Seaton, M. A., Anderson, R. L., Metz, S., & Smith, W. DL_MESO: highly scalable mesoscale simulations. *Molecular Simulation* (2013) **39**: 796-821.